Multisource emission retrieval within a biogas plant based on inverse dispersion calculations—a real-life example

Marlies Hrad, Martin Piringer, Ludek Kamarad, Kathrin Baumann-Stanzer & Marion Huber-Humer

Environmental Monitoring and Assessment
An International Journal Devoted to Progress in the Use of Monitoring Data in Assessing Environmental Risks to Man and the Environment

ISSN 0167-6369

Environ Monit Assess
DOI 10.1007/s10661-014-3852-0

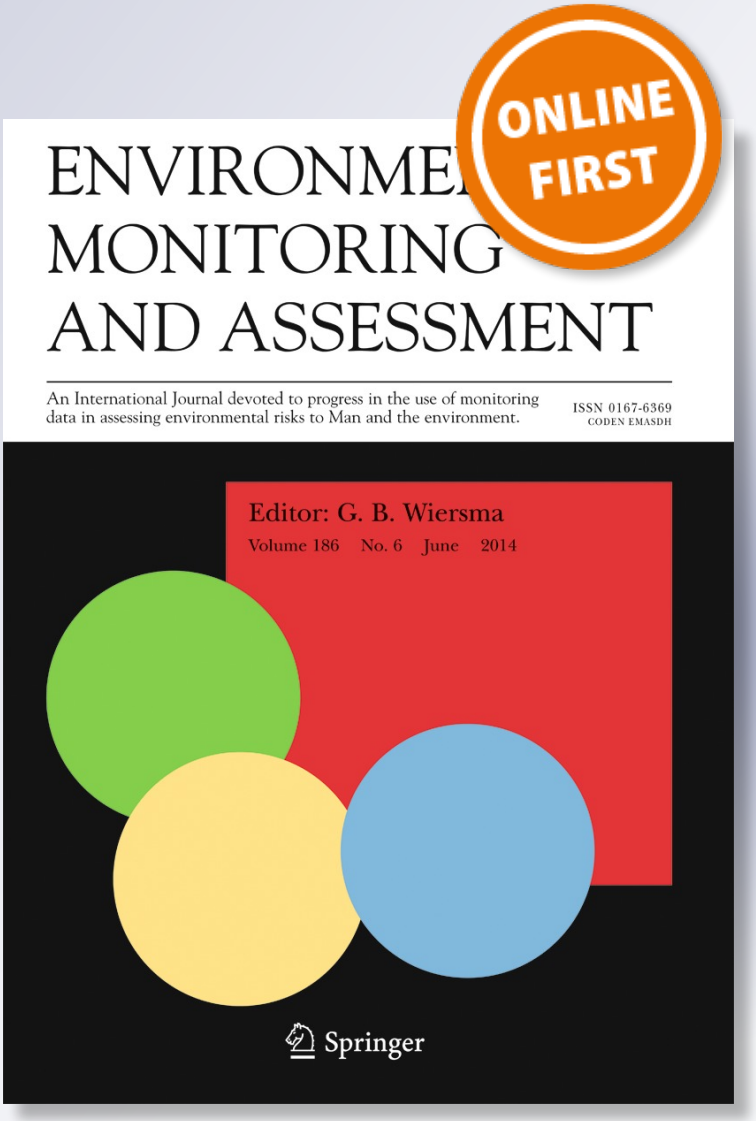

Springer

Environ Monit Assess
DOI 10.1007/s10661-014-3852-0

Multisource emission retrieval within a biogas plant based on inverse dispersion calculations—a real-life example

Marlies Hrad · Martin Piringer · Ludek Kamarad · Kathrin Baumann-Stanzer · Marion Huber-Humer

Received: 19 November 2013 / Accepted: 21 May 2014

Abstract Open digestate storage tanks were identified as one of the main methane (CH_4) emitters of a biogas plant. The main purpose of this paper is to determine these emission rates using an inverse dispersion technique in conjunction with open-path tunable diode laser spectroscopy (OP-TDLS) concentration measurements for multisource reconstruction. Since the condition number, a measure of "ill-conditioned" matrices, strongly influences the accuracy of source reconstruction, it is used as a diagnostic of error sensitivity. The investigations demonstrate that the condition number for a given source-sensor configuration in the highly disturbed flow field within the plant significantly depends on the meteorological conditions (e.g., wind speed, stratification, wind direction, etc.). The CH_4 emissions are retrieved by removing unrepresentative periods with high condition numbers, which indicate uncertainty in recovering the individual sources. In a final step, the CH_4 emissions are compared with the maximum biological methane potential (BMP) in the digestate analyzed under laboratory conditions. The retrieved methane emission rates represent an average of 50 % of the maximum BMP of the stored digestate in the winter months, while they comprised an average of 85 % during the measurement campaigns in the summer months. The results indicate that the open tanks have the potential to represent a substantial emission source even during colder periods.

Keywords Optical remote sensing technique · Multisource reconstruction · Lagrangian dispersion model · Condition number · Open digestate storage tank · Methane emissions

M. Hrad (✉) · M. Huber-Humer
Department of Water-Atmosphere-Environment, Institute of Waste Management, University of Natural Resources and Life Sciences,
Muthgasse 107, 1190 Vienna, Austria
e-mail: marlies.hrad@boku.ac.at

M. Piringer · K. Baumann-Stanzer
Department of Environmental Meteorology, Institute for Meteorology and Geodynamics,
Hohe Warte 38, 1190 Vienna, Austria

L. Kamarad
Department for Agrobiotechnology, Institute for Environmental Biotechnology, University of Natural Resources and Life Sciences,
Konrad-Lorenz-Straße 20, 3430 Tulln, Austria

Introduction

Biogas plants can contribute to the reduction of greenhouse gases (GHG), and, therefore, play an important role in meeting national as well as international environmental targets. The environmental benefits of using biogas primarily stem from the substitution of fossil energy. However, the net GHG reduction from a facility will be heavily impacted by any fugitive CH_4 losses during production. Digestate storage tanks without a gas-tight cover were identified as one of the main CH_4 emitters (Edelmann et al. 2001; Liebetrau et al. 2010). Digestate is produced throughout the year and must, therefore, be stored for a specific amount of time (regulated by national law) until the appropriate time for its

Published online: 29 May 2014

application on fields as a fertilizer. The accurate determination of average emissions caused by open storage facilities is quite challenging. Different approaches have been made involving floating chambers that are applied directly on the liquid surface in order to quantify the remaining gas emission of the digestate under field conditions (Liebetrau et al. 2010). Since the emissions from digestate tanks depend on meteorological conditions (e.g., wind, temperature, atmospheric pressure, etc.), the filling level of the tank and the process efficiency of the digester, traditional point monitoring measurements (e.g., surface chamber, portable methane detector) have a limit with respect to the spatial and temporal resolution of these emissions. Up to now, data on CH_4 emissions from open storage tanks is scarce and, therefore, the relevance of these losses demonstrating the actual plant efficiency has not been well-evaluated (Liebetrau et al. 2010; Siegl et al. 2011).

In recent years, numerous international studies have demonstrated the potential of micrometeorological (e.g., numerical dispersion models) or tracer techniques (e.g., static or dynamic plume monitoring) using ground-based optical remote sensing (ORS) (Flesch et al. 2005, 2011; Goldsmith et al. 2012). ORS technologies utilize open-path spectroscopic instrumentation, such as open-path Fourier transform infrared (OP-FTIR), ultraviolet differential absorption spectroscopy (UV-DOAS) or open-path tunable diode laser spectroscopy, to obtain line-averaged pollutant concentration information downwind from the source. In comparison to point monitoring approaches, micrometeorological or tracer techniques in conjunction with ORS-based concentration measurements provide higher spatial and temporal resolution of concentration data, allowing for characterization of emission plumes and the calculation of emission fluxes. Such techniques have been used to characterize fugitive emissions from large area sources including landfills (Galle et al. 2001; Scheutz et al. 2011; Goldsmith et al. 2012), agricultural operations (Flesch et al. 2005; McGinn et al. 2006, 2009, 2011), and biodigesters (Flesch et al. 2011).

When measurements are applied in the vicinity of a single source, emission rates can be quantified with an uncertainty less than 10–20 % (Flesch et al. 2004, 2005). A simple approach to reconstruct the emission time series for one source using an inverse dispersion technique is described by Flesch et al. (2005) and later applied, e.g., by Schauberger et al. (2011) for odor emissions from a waste treatment plant (Eq. 2). However, biogas plants are a composite of sources and, therefore, represent a multisource problem, in which n concentration sensors are located in proximity to m sources, each source having its own emission rate. A best case scenario implies that each concentration sensor is placed so as to detect only one source at a time (Crenna et al. 2008; Flesch et al. 2009). In the real world, it can be quite difficult to make isolated measurements of emissions from these sources due to the practical limitations of sensor placement or the need to accommodate a range of wind directions.

In general, inverse multisource reconstruction can be undertaken in different ways. Flesch et al. (2009) proposed a method to solve multisource problems, where the number of (line-average) concentration sensors (n) equals that of the emission sources (m) which are to be determined ($m \times n$ matrix). The "least square method," a statistical best fit approach, is similar and applied to an overdetermined problem where the number of sensors exceeds the number of sources. In the case of multisource problems, in which the number of sources is unknown a priori, Bayesian probability theory is taken to derive the posterior probability density function for the sources under investigation and the parameters that characterize each source (Yee 2008; Yee and Flesch 2010).

The main objective of this paper is to quantify the source strengths ($m \times n$ matrix) of three open digestate storage facilities and two pig manure tanks within a biogas plant from selected measurement days using a wind flow model to drive the dispersion calculations. The retrieved emission rates from the concentrations measured by the OP-laser are compared with the theoretically possible methane emissions of the digestate analyzed under laboratory conditions (samples taken directly from an open storage tank during concentration measurements).

Material and methods

Biogas generation at the study site

The biogas facility operates adjacent to a pig breeding farm and processes energy crops and pig manure for co-digestion. About 11,000 t of energy crops, which mainly consist of maize silage and small amounts of by-products from vegetable processing, together with 7,300 t of liquid pig manure are

processed annually in two parallel digesters (mesophilic; hydraulic retention time in the closed system 80–100 days including the gas-tight final digestate storage tank; in heated digester about 60 days) and a gas-tight final digestate storage tank. Since the application of digestate on farmland as a fertilizer is not allowed during winter (November–February) in Austria, the fermentation residues are stored in three open storage tanks (total volume 3,800 m^3) (sources Q2, Q3, and Q5 in Fig. 1) once the capacity of the gas-tight final storage tank (2,000 m^3) is exceeded. Depending on the weather conditions, the maximum retention time of digestate in the open storage tanks can achieve more than 120 days. Until the co-digestion of pig manure, the liquid substrate is stored in two underground tanks (total capacity 1,200 m^3) (sources Q1 and Q4 in Fig. 1). The generated biogas (about 4,020,000 m^3/year) is utilized in two combined heat and power units with an installed capacity of 1 MW electric energy and 1.034 MW thermal energy.

Concentration measurements

Methane concentration measurements were performed using an open-path tunable diode laser spectroscopy (OP-TDLS) system (GasFinder 2.0, Boreal Laser Inc., Edmonton, Canada). The CH_4 laser was automatically aligned to multiple reflectors in order to collect path-integrated gas concentration data along multiple beam paths. The open-path laser was, therefore, mounted on a digital scanning motor (Model PTU D300, Directed Perception Inc., CA, USA) which was remotely controlled using available hardware and software (Boreal Laser Inc.). The path-integrated (line-average) CH_4 concentrations were recorded every second (average of 256 measurements per second) for 60 s along each path. The concentration data was averaged over 10-min periods. Measurements were performed during daytime operation of the plant. Due to varying setup times and occasional equipment malfunctions, the measurement campaign lasted between 3 and 6 h. The seven retro reflectors were mounted on tripods at a height of 2 m

Fig. 1 Sources (*Q1*, *Q4*: covered pig manure storage tanks; *Q2*, *Q3*, *Q5*: open digestate storage tank; release height 0.1 m), laser paths (18–89 m), picture and location (*white dot*) of the ultrasonic anemometer at the biogas plant (north-orientated)

according to Fig. 1. The laser was positioned at a height of 1.5 m. Path lengths ranged from 18 to 89 m. Background CH_4 concentration was measured at least once a week over the period of 1 year with the laser upwind of the biogas plant.

Meteorological measurements

Continuous meteorological measurements with a three-dimensional (3D) ultrasonic anemometer (taken over a period of 1 year) provide the wind and turbulence data base for the dispersion model. At the study site, the 3D sonic anemometer (Model uSonic-3 Scientific, Metek GmbH, Elmshorn, Germany) was located at the northeast edge of the substrate storage during the study (see Fig. 1). The anemometer was mounted on top of a 10-m-high mast above the soil surface to measure key wind and turbulence parameters needed for the dispersion model. The components of the wind vector (x, y, z) and the sonic temperature were measured at 10 Hz. Atmospheric stability was determined from the optimal sensor placement (OSP) in (m^{-1}), the inverse of the Obukhov length L, deduced from the wind statistical data collected by the 3D anemometer. L has been calculated by the software associated with the anemometer. The OSP was calculated according to the following equation,

$$\mathrm{OSP} = \frac{-\kappa g \overline{z'T'}}{u*^3 \overline{T\mathrm{k}}} \tag{1}$$

where κ is the Kármán constant (0.37), g is the acceleration due to gravity (9.81 ms^{-2}), $u*$ defines the friction velocity, T_k describes the temperature in Kelvin, and the term $\overline{z'T'}$ is the covariance of the vertical component of the wind (z) and the temperature (T).

In general, positive values of OSP indicate stable atmospheric conditions, while negative values are classified as unstable. OSP values near zero indicate neutral conditions. All data was averaged into 10-min values. Due to the complex array of building obstacles of different sizes, the surface roughness length (z_0) was assumed to be 1 m.

Lagrangian particle diffusion model

The dispersion model Lagrangian Simulation of Aerosol Transport (LASAT) (Janicke Consulting 2011) simulates the dispersion and the transport of a representative sample of tracer particles utilizing a random walk process (Lagrangian simulation). It computes the transport of passive tracer substances in the lower atmosphere (up to heights of about 2,000 m) on a local and regional scale. LASAT includes a mass-consistent diagnostic wind field model which accounts for enhanced turbulence and recirculation effects around buildings. The model can use the complete meteorological and turbulence information of a 3D ultrasonic anemometer. Atmospheric stability is directly deduced from the measured turbulence (Obukhov length). LASAT has been evaluated with a series of international test data sets including the Prairie Grass and Copenhagen experiments, investigations at the Nuclear test facility Karlsruhe in Germany, as well as experiments in complex terrain (Hirtl and Baumann-Stanzer 2007; Hirtl et al. 2007; Baumann-Stanzer et al. 2008; Piringer and Baumann-Stanzer 2009; Schatzmann et al. 2010).

The configuration depicted in Fig. 1 is used to quantify sources Q1 to Q5 by selecting the appropriate path depending on the prevailing wind direction. Using line concentration sensors, it is not possible to detect only one source at a time. The measurement setup was, therefore, selected according to recommendations by Flesch et al. (2009), where the most successful scenario was a "progressive" layout. In this case, source 1 is isolated with the first path; the second path "sees" the blended plume from sources 1 and 2, and so on. The location of the laser was chosen in order to minimize the disturbance of the plant operation. Since LASAT cannot represent line concentration sensors, a set of "monitoring points" was placed along each path taking the maximum concentration for the emission retrieval. The resolution is 1 point/m, in accordance with the model grid resolution. In the model grid cell with the maximum concentration along the path, 100 particles per second were released for the emission retrieval.

Inverse multisource strength reconstruction and condition number

The emission rate Q for a single source is calculated from the measured gas concentration C (above background) and the dispersion model prediction of the ratio of concentration at the sensor to the emission rate $(C/Q)_{sim}$.

$$Q = \frac{C}{(C/Q)sim} \tag{2}$$

The application of the method for a multisource problem, as in the current case, is done with a set of linear equations as described in detail in Flesch et al. (2009) which requires at least as many (line-averaged) concentration sensors as sources. For two emission rates Q1 and Q2 and two receptors A and B, the appropriate equation in matrix notation is

$$\begin{bmatrix} (CA,1/Q1)sim & (CA,2/Q2)sim \\ (CB,1/Q1)sim & (CB,2/Q2)sim \end{bmatrix} \begin{bmatrix} Q1 \\ Q2 \end{bmatrix} = \begin{bmatrix} CA \\ CB \end{bmatrix} \tag{3}$$

The condition number κ is a measure of "ill-conditioning," i.e., if the solution is extremely sensitive to changes in the input data (measurements or model estimates), and for the above matrix is given by (Gerald and Wheatley 1984)

$$\kappa = \|(C/Q)sim\| * \left\|(C/Q)sim^{-1}\right\| \tag{4}$$

In general, the condition number of a matrix measures how small perturbations in the input affect the results. If the matrix is well-conditioned, then small changes in the input produce small changes in the results. If small changes in the input lead to large changes in the output, then the matrix is ill-conditioned. The exact cutoff line between well- and ill-conditioned matrices depends on the context of the problem and the uses of the results. Flesch et al. (2009) proposed certain κ limits derived from a particular study layout and meteorological conditions. Source decomposition was possible if κ<10–20; for the total emission of all sources, κ<50 assuming ideal terrain.

The error in the emission reconstruction ε_Q can be as large as the sum of the measurement (ε_C) and modeling error ($\varepsilon_{C/Q}$) multiplied by the condition number[1] (Crenna et al. 2008; Flesch et al. 2009):

$$\frac{\|\varepsilon Q\|}{\|Q\|} \leq \kappa \left(\frac{\|\varepsilon C/Q\|}{\|(C/Q)sim\|} + \frac{\|\varepsilon C\|}{\|C\|} \right) \tag{5}$$

. In the specific study of Flesch et al. (2009), the uncertainty in the dispersion model prediction $(C/Q)_{sim}$ was 10–20 %. It should be noted that in real-world situations—as in this case—the level of model uncertainty may be higher. Flesch et al. (2009) found that the accuracy of calculating total emissions was 90 % on average (average κ of 4.2), while there was higher uncertainty in the individual source inferences. The accuracy of the multisource reconstruction declined rapidly for the layouts with high κ values (where it was not possible to isolate any source).

[1] It should be noted that some problems with unreasonably large κ values suffer from "artificial" ill-conditioning due to a "badly scaled" matrix (Gentle 1998). In this case, a large value of κ does not guarantee sensitivity to error.

Laboratory investigation

Representative digestate samples were taken on selected days from the open storage tank Q3 (Fig. 1) during the OP-TDLS concentration measurements. The biological methane potential (BMP) was determined at 35 °C without addition of inoculum according to German standard VDI 4630 and DIN 38 414-S8. Each test run lasted for 140 days to identify the maximum BMP of digestate in the storage tank under ideal conditions taking into account typical retention times (over 120 days). The total volatile solids (TVS) and total solids (TS) were determined according to DIN 38 409- H1-3 and DIN 38 409- H1-1. The chemical oxygen demand (COD) was analyzed according to DIN 38 409 - H41 and ÖNORM M 6265. Volatile fatty acids (VFA) concentrations in the digestate were monitored as well. No significantly high VFA concentrations were detected indicating a stable anaerobic digestion process without any biological process inhibition.

The potential methane emission rate (Nm^3 CH_4/h) was calculated using the measured BMP, the effective digestate volume of the tank and the volatile solids contained in the digestate. Within the selected storage tank Q3 (max. capacity 600 m^3), a measuring scale (measuring step 0.5 m) was attached in order to determine the filling level of the tank. The BMP potential of the sediment layer in the storage tank (approx. 0.15 m) was analyzed as well and added to the individual BMP of the selected days. Data of the basic digestate characterization used for the model validation is presented in Table 1.

Results and discussion

Wind data, atmospheric stability, and modeled wind field

The site experiences average wind speeds of about 3 m s^{-1}, and the distribution of wind directions and wind

Table 1 Digestate characteristics

Date	TS (%)	TVS (%)	VFA (mg/l)	COD (g/kg)	BMP (Nm^3 CH_4/ Mg wm)	Filling level (m^3) (Q3)
13.12.2011	3.2	2.2	109	32.5	2.4	60
23.02.2012	6.8	5.1	205	76.4	8.8	540
06.03.2012	6.8	5.1	133	80.4	7.1	400
26.04.2012[a]	10.2	5.8	930	97.4	6.6	30
10.07.2012	5.5	4.9	58	62.9	4.7	540
18.08.2012	4.4	3.2	71	57.9	3.3	480

TS total solids, *TVS* total volatile solids, *VFA* volatile fatty acids, *COD* chemical oxygen demand, *BMP* biological methane potential, *wm* wet mass

[a]Sediment/bottom

speeds during daytime is shown in Fig. 2a. Winds from southwest are most common and show also a considerable fraction of speeds above 7 m s^{-1}. In anticyclonic conditions often occurring on the sampling days, easterly winds are quite frequent. Both wind direction segments are favorable for the orientation of the laser paths (Fig. 1).

Atmospheric stability is analyzed via the Obukhov stability parameter (m^{-1}) deduced from data collected by the 3D ultrasonic anemometer, the inverse of the Obukhov length. The limit values to discern different stability conditions are "unstable<−0.005<neutral< 0.002<stable" (m^{-1}), for an assumed roughness length of z_0=1 m. Stable cases (gray in Fig. 2b) occur seldom during daytime, as expected, and are restricted to the hours around sunrise and sunset. Southwesterly winds are predominantly connected with neutral atmospheric stability (white in Fig. 2b), whereas unstable conditions (black in Fig. 2b) dominate with easterly winds.

Biogas plants usually consist of a complex building structure which might be challenging for the determination of emission fluxes from plant components, such as open digestate storage tanks. Given the complexity in wind flow amongst the building and structures of the biogas plant (where the concentration measurements are conducted), the authors have taken the view that resolving this complex flow is an important part of this analysis, although this view might not be universally accepted. Wilson et al. (2010) describes the challenges associated with resolving complex flow, and how this complexity can compromise the accuracy and flexibility of the inverse dispersion technique. However, the authors recognize the potential benefit to modeling a complex flow when concentration sensors are located in an area of highly disturbed winds, as in this situation.

The wind field is simulated for diverse meteorological conditions using different wind directions and atmospheric stability conditions. As can be seen in Fig. 3, the wind field model associated with LASAT recognizes the presence of the main wind obstacles when calculating the flow field and the result is plausible. The approach flow in this example is from NE and the atmospheric

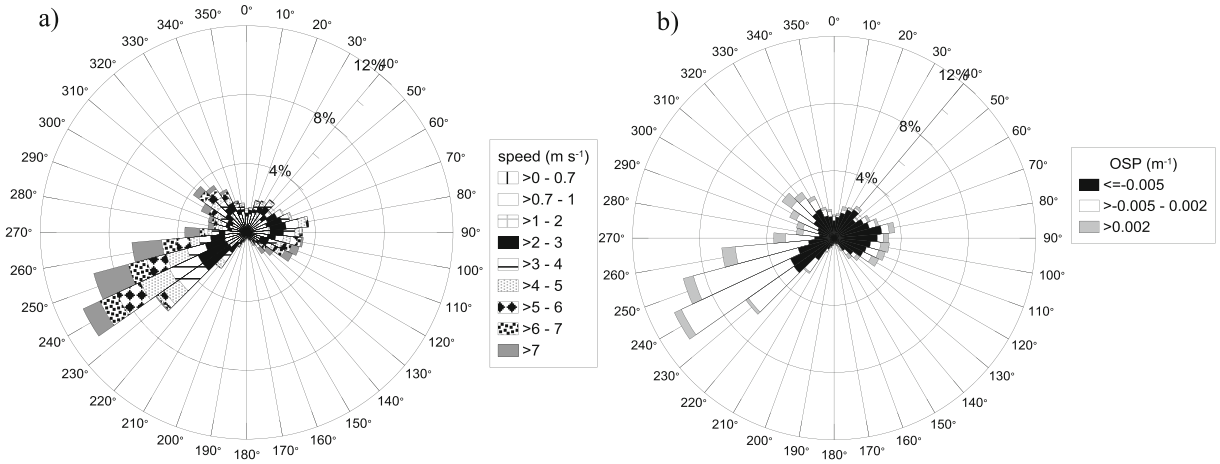

Fig. 2 Daytime wind rose (**a**) and daytime OSP (**b**) (average from 13.09.2011 to 21.01.2013) measured by the 3D ultrasonic anemometer at the biogas plant

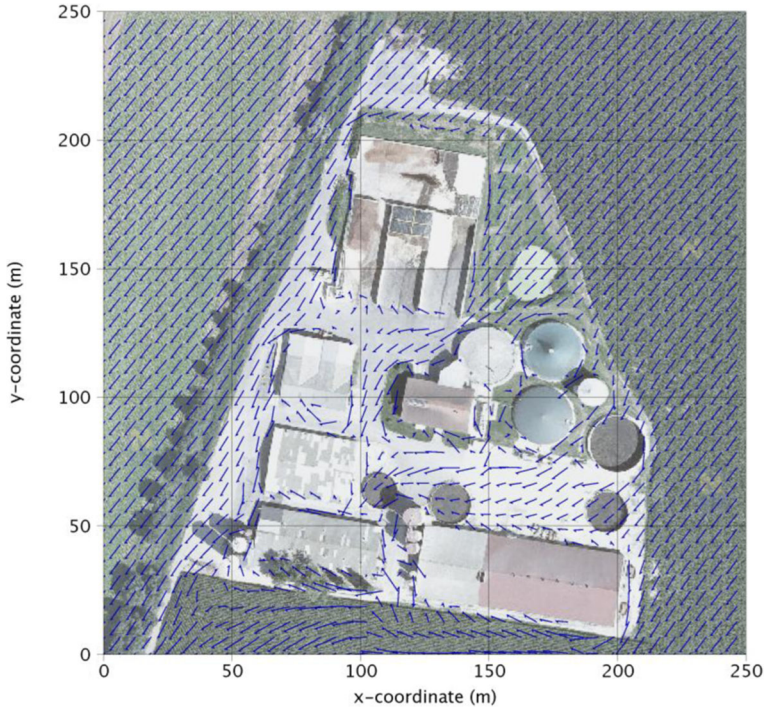

Fig. 3 Example of the wind field within the biogas plant calculated with LASAT for an approach flow from NE at a height of 2 m above ground

stability is neutral. The flow between the buildings and the containers at a height of 2 m above ground is considerably disturbed: it is partly channeled and partly reversed, and in the lee of some buildings, wake areas are seen.

Multisource emission retrieval

The inverse dispersion technique is used to relate measured concentrations by the OP-laser to the individual sources (Q1–Q5) for the applied source-sensor geometry (relative positioning between sensors and sources) at selected measurement days. The area sources Q2, Q3, and Q5 represent open digestate storage tanks. In contrast, sources Q1 and Q4 consist of closed tanks of liquid pig manure, which only have small openings for the stirrer (Fig. 1). These point sources are identified as weak potential emitters using a portable flame ionization detector during first site inspections. The selected days are listed in Table 2 together with a short characterization of the meteorological conditions and the number of observed 10-min periods (n). Other potential emission sources of the biogas plant (e.g., safety valves, flare, point leakages at gas-tight covers, etc.) are not considered since they have been mainly identified as short-termed and temporal sources (using the OP-laser). This was also periodically verified using a portable flame ionization detector. Because of the confined location of these sources, multisource emission retrieval was not possible.

Diagnostic tool "condition number"

Since multisource problems tend to be mathematically ill-conditioned, the condition number of a matrix κ has been proven helpful as a diagnostic of error sensitivity (Crenna et al. 2008, Flesch et al. 2009). Based on a field study with four synthetic emission sources on a flat terrain, Flesch et al. (2009) proposed certain κ limits for individual source inferences (κ<10–20) and for calculating total emissions (κ<50).

The parameter κ was, therefore, used to assess the error sensitivity of the applied source-sensor geometry at different meteorological conditions. Figure 4 depicts the dependence of the condition number on the wind speed, wind direction, and the OSP parameter for all experimental days. Each 10-min period has a unique κ determined by the source-sensor geometry and wind conditions. In summary, 64 % of the condition numbers were found well below 20, and 82 % below 50. Of all meteorological parameters investigated, the dependence of the condition number on wind speed is the strongest:

Table 2 Short characterization of the days of the experiment

Date	∅ Wind direction	∅ Wind speed	Stability	Digestate sample	*n* 10-min values	Comment
13.12.2011	SE, N, SW	1.7 m s^{-1}	Variable	x	36	Q2, Q3, and 5 empty
23.01.2012	WSW	7.0 m s^{-1}	Neutral	x	40	Q2, Q3, and 5 filled
24.01.2012	WNW	5.5 m s^{-1}	Neutral	x[a]	37	Q2, Q3, and 5 filled
08.02.2012	NE-SE	2.5 m s^{-1}	Variable		20	Q2, Q3, and 5 filled
06.03.2012	NE-E	2.5 m s^{-1}	Unstable	x	32	Q2, Q3, and 5 partly emptied since 15.02
10.07.2012	SE	2.0 m s^{-1}	Unstable	x	31	Only Q3 filled
16.08.2012	SW	3.0 m s^{-1}	Neutral	x	31	Only Q3 filled

[a] Same sample as 23.01.2012

large condition numbers (values of κ>20) indicating uncertainty in recovering the sources are found for wind speeds below 4 m s^{-1} only (Fig. 4a). The latter are mainly associated with experimental days 1 and 4 to 6 on which wind speeds were lowest on average. The dependence of κ on wind direction (Fig. 4b) and atmospheric stability (Fig. 4c) is less clear compared to wind speed (Fig. 4a), but some conclusions can be drawn. Crenna et al. (2008) found a significant variation of κ with stability besides the sensor arrangement, whereas the quality of emission reconstruction did not depend on meteorological conditions in a field study from Flesch et al. (2009), most probably because unfavorable wind conditions have been excluded from the analysis. Ill-conditioning (values of κ>20) is more common, for the on average weaker easterly winds, than for the stronger

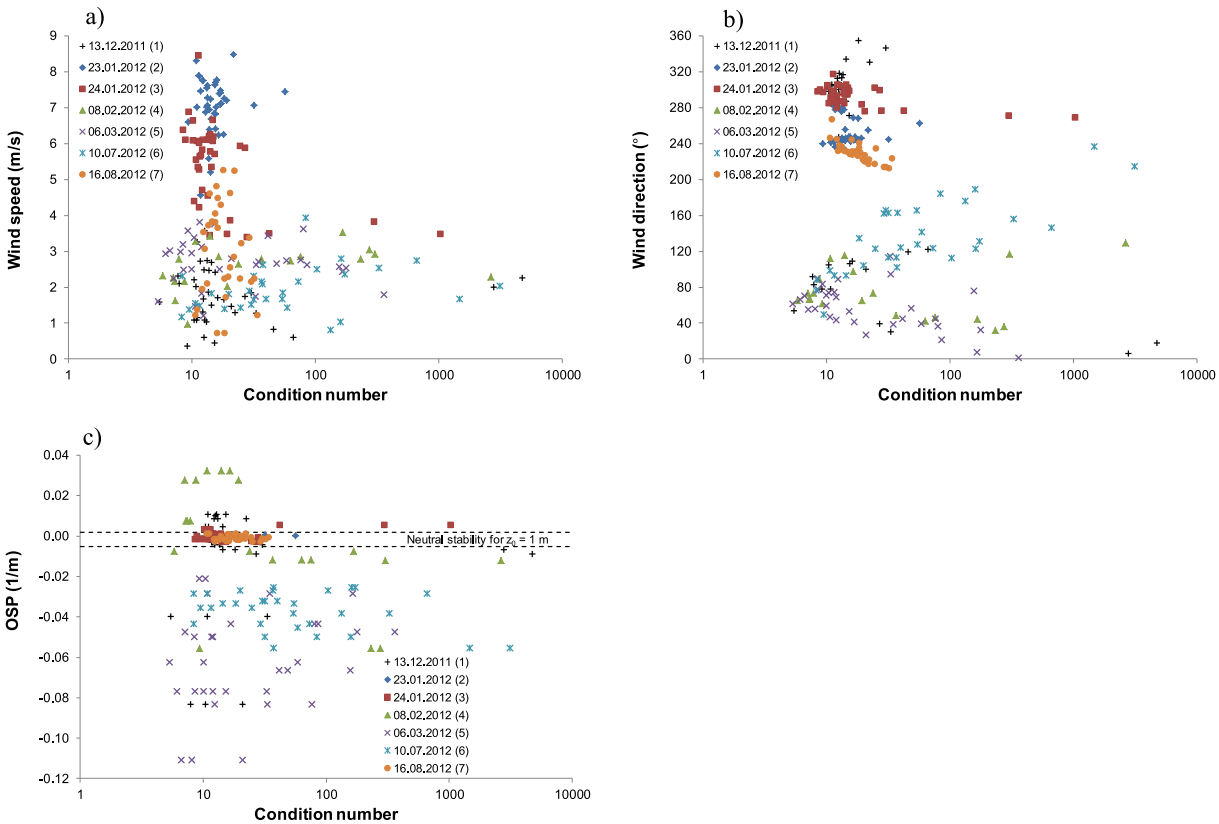

Fig. 4 Dependence of the condition number κ on the wind speed (**a**), wind direction (**b**), and the OSP parameter (**c**) for all experimental days

westerly winds (Fig. 4b). In addition, it occurs much more frequently in unstable conditions than in neutral or stable ones.

The 3 days with neutral stratification show mostly low condition numbers, even with weak winds on day 7. In neutral conditions, possible reasons of uncertainty, namely short-term up- and downdrafts of plumes caused by buoyancy in unstable or wind shear in stable conditions, should be absent or play a minor role, thus improving model predictions. As instability and weak winds frequently occur on the same days (days 1, 5, and 6 of the experiment), this combination is most likely to give rise in uncertainties of the algorithm to discriminate between single sources.

In Fig. 5, the dependence of κ on the methane emission rate of each source is exemplarily displayed for the days 2 (most values of $\kappa<20$) and 6 (most values of $\kappa>20$). Experiment day 6 has very large condition numbers resulting in negative emissions rates (down to -107 Nm^3/h) and unreasonably large positive values (up to 155 Nm^3/h) of sources Q4 and Q5 (Fig. 5b). This effect is less pronounced for experiment day 2 with stronger westerly winds and neutral atmospheric conditions. Similar results were found by Flesch et al. (2009), where emission variability and bias increased with greater κ values. Negative emission values imply that an emission sink, which absorbs target gas within the area, best explains the observations (Flesch et al. 2009). However, this is an unrealistic outcome which represents a problem of the mathematical solution (nothing precludes negative emissions). In order to avoid the potential of negative emissions, one could apply a constrained iterative approach that minimizes the sum of the square errors of the metric (Flesch et al. 2009).

Removing unrepresentative periods

Since the accuracy of multisource determination depends strongly on the condition number (Flesch et al. 2009), various approaches have been examined to handle the problem of ill-conditioning in equations relating source emission rates to concentrations (Roussel et al. 2000; Haupt et al. 2006). Crenna et al. (2008) recommend an increase of the number of measurements by either adding more sensors or by incorporating data taken over a longer time period in order to overcome the effect of large κ values. However, adding an arbitrary number of poorly located sensors will be of little or no benefit (Crenna et al. 2008). Since concentration measurements have been taken over several hours (see Table 2), in this case, ill-conditioned periods (values of $\kappa>20$) are simply removed to reduce the significance of particular measurement periods. In Table 3, the numbers of remaining 10-min periods after the filtering process are presented. In addition, Table 3 shows the retrieved methane emission rates of the component sources Q1–Q5 as well as the total CH_4 emissions in comparison with the potential CH_4 emission of the digestate in Q3 analyzed under laboratory conditions ("Sample" in Table 3). The retrieved emission rates of sources Q1 and Q4 ranged between 0 and 0.3 Nm^3 CH_4/h representing a minor source strength compared to Q2, Q3, and Q5, which could be also confirmed by the first site inspection using a portable flame ionization detector. It should be noted that a direct comparison of the retrieved emission rates between sources Q2, Q3, and Q5 is limited due to the diverse filling times of the tanks. In addition, Q2 and Q5 were empty on measurement days 1, 6, and 7 (as already mentioned in Table 2) apart from the sediment diluted with rainwater during the summer measurements. The retrieved emission rates of Q2 and Q5 varied between 0 and 0.3 Nm^3 CH_4/h during this time. In comparison, the sediment in the tanks had a BMP of 0.1 Nm^3 CH_4/h under laboratory conditions. During the experiment days 2 to 4, Q2, Q3, and Q5 represented the dominant sources ranging from 0.5 to 1.0 Nm^3 CH_4/h, while Q3 had the greatest source strength (0.6–0.8 Nm^3 CH_4/h) during the summer measurements (experiment days 6 and 7). Since all three open digestate tanks (Q2, Q3, and Q5) were filled during the experiment days 2–4 and only Q3 during the days 6 and 7, the source reconstruction is considered as plausible.

In order to check the plausibility of source reconstruction, the retrieved emissions rates were compared with the potential CH_4 emission of the digestate in Q3. It is important to note, that the laboratory tests determining the BMP were carried out under idealized conditions at 35 °C. The temperature in the storage tank in fact did not exceed 30 °C. The lowest measured temperature in the tank was 8 °C. Since the storage temperature of the digestate has a great influence on the emissions, it can be assumed that the actual methane emissions are lower because of reduced biological activity at lower temperature in the digestate storage tank. Several laboratory studies have indicated that the emission potential is reduced significantly depending on the temperature of the digestate during storage (Liebetrau et al. 2011; Reinhold et al. 2010; FNR 2009). Liebetrau et al.

(2011) showed that the average methane potential obtained at 20 °C is reduced to 39 % of the value obtained at 39 °C. Reinhold et al. (2010) found an average reduction of the methane production of 50–60 % by decreasing the temperature from 37 to 25 °C, while the methane potential decreased further to even 1 % at 10 °C. In this study, the retrieved methane emission rates from the concentrations measured by the OP-laser represented an average of 50 % of the maximum emission potential in the digestate in the winter months, whereas they comprised an average of 85 % in the summer months. The results indicate that the open tanks have the potential to represent a substantial emission source even during colder periods. As can be seen in Table 1, the BMP of the digestate samples ranges between 2.4 and 8.8 Nm^3 CH_4/Mg wet mass and is in

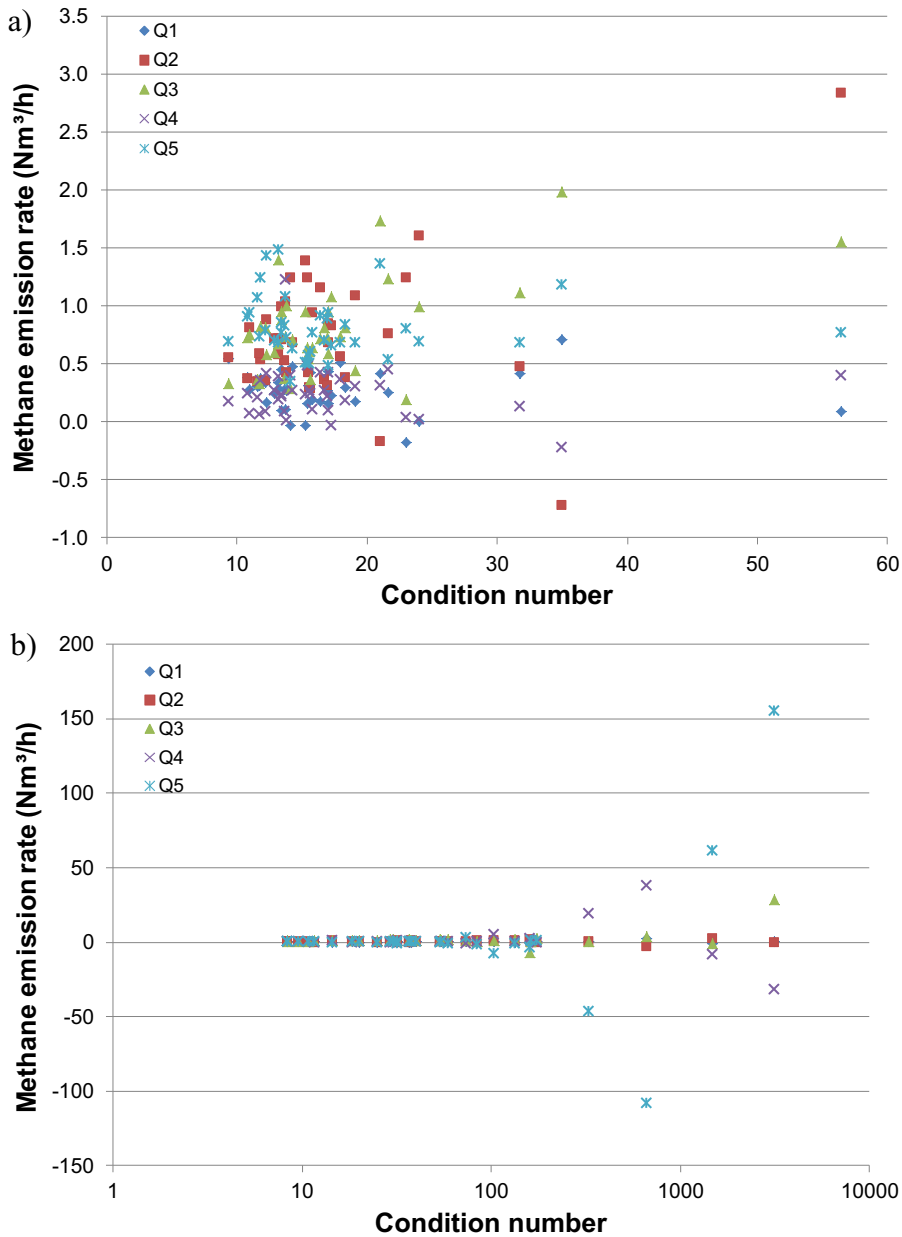

Fig. 5 Dependence of the condition number κ on the retrieved methane emission rate in Nm^3/h of experiment day 2 (**a**) and day 6 (**b**); it should be noted that each plot has different scale on its vertical and horizontal axes

Table 3 Retrieved median methane emission rates vs. maximum emission potential in the digestate at 35 °C in Nm^3 CH_4/h (Sample Q3)

Date	*n*	Q1	Q2	Q3	Q4	Q5	Total	Sample (Q3)
13.12.2011	11	0.0 (0.0)	0.0 (0.0)	0.0 (0.1)	0.0 (0.0)	0.1 (0.0)	0.2 (0.1)	0.1
23.01.2012	30	0.3 (0.1)	0.5 (0.2)	0.7 (0.2)	0.2 (0.1)	0.8 (0.2)	2.5 (0.3)	1.5
24.01.2012	21	0.1 (0.0)	0.5 (0.2)	0.8 (0.2)	0.1 (0.1)	0.9 (0.2)	2.4 (0.3)	1.5
08.02.2012	9	0.3 (0.1)	0.9 (0.2)	1.0 (0.4)	0.3 (0.3)	0.7 (0.2)	3.4 (0.9)	–
06.03.2012	17	0.1 (0.1)	0.3 (0.2)	0.5 (0.1)	0.2 (0.1)	1.0 (0.3)	2.1 (0.6)	0.8
10.07.2012	6	0.2 (0.1)	0.2 (0.1)	0.8 (0.2)	0.2 (0.1)	0.3 (0.1)	1.5 (0.2)	0.9
16.08.2012	16	0.2 (0.0)	0.3 (0.1)	0.6 (0.2)	0.2 (0.0)	0.2 (0.1)	1.5 (0.3)	0.7

Standard deviations are given in brackets (); *n* indicates the amount of remaining 10-min periods

the same order of magnitude as investigations conducted by Liebetrau et al. (2010, 2011) and Reinhold et al (2010). Since other potential sources within the biogas plant (e.g., safety valves at gas storage, point leakages at gas-tight covers, barns) are disregarded in this study, they might have influenced the concentration measurements conducted at sources 1–5, in particular at northeasterly winds.

Conclusions

For a biogas plant, CH_4 source reconstruction was undertaken by a combination of ground-based ORS (OP-TDLS) and an inverse dispersion technique resolving the complex building structure and incorporating different kinds of sources. The algorithm of source identification is based on investigations by Flesch et al. (2009) and was applied here for a real-world industrial setting. The condition number, as a measure of ill-conditioned matrices, was used as a diagnostic of error sensitivity. The investigations demonstrated that the condition number for a given source-sensor geometry in a complex building environment depends on atmospheric stability, wind direction, as well as wind speed. Lower condition numbers ($\kappa<20$) were mainly found for larger wind speeds and neutral atmospheric stability indicating a higher accuracy for multisource retrieval during these conditions. Since concentration measurements have been taken over several hours, ill-conditioned periods (values of $\kappa>20$) were simply removed for emission retrieval. By applying this method, average methane emissions were obtained limiting a comprehensive representation of temporal emission variation, especially for experiment days 1, 4, and 6. The cutoff values of the condition number were based on a specific study layout and meteorological conditions assuming ideal terrain (Flesch et al. 2009). It should be noted, that in real-world situations with disturbed wind fields—as in this case—the level of model uncertainty may be higher as in the study of Flesch et al. (2009). In future studies, the multisource reconstruction could be further tested and verified releasing tracer gases with known rates at each source within the disturbed wind field of the biogas plant.

Changes in meteorological conditions during a measurement campaign will make sensor placement increasingly difficult as also shown by Crenna et al. (2008). In order to optimize the line-sensor placement for each measurement day, a numerical model could assess the response of condition number to a given sensor arrangement under different atmospheric conditions. However, in practice, separating multiple sources may be not possible in some cases because sensors would have to be frequently repositioned to accommodate changes.

In order to check the plausibility of the inverse multisource determination, the retrieved methane emissions were compared with the maximum BMP of the digestate at 35 °C analyzed under optimal laboratory conditions. Results indicate that temperature has a great influence on the emissions, and open digestate storage tanks are potential methane emitters even during colder periods. The significantly higher VFA concentration measured in the sediment sample (26.04.2012) could indicate a higher biological activity on the bottom of the tank compared to the rest of the total storage tank volume.

Acknowledgments These investigations were part of the research project "KLIMONEFF," which was funded by the Austrian "Klima- und Energiefonds - Neue Energien 2020." The applied measurement equipment was made available in cooperation with EQ Equipment BOKU Vienna Institute of Biotechnology GmbH.

References

Baumann-Stanzer, K., M. Piringer, E. Polreich, M. Hirtl, E. Petz, M. Bügelmayer, (2008). *User experience with model validation exercises. Ext. abstract of the 12th Int. Conf. on harmonization within atmospheric dispersion modeling for regulatory purposes*, Cavtat, Croatia, 6 – 10 Oct. 2008. In: Croatian Meteorological Journal 43, Vol. 1, 52 – 56, ISSN 1330-0083.

Crenna, B. P., Flesch, T. K., & Wilson, J. D. (2008). Influence of source-sensor geometry on multi-source emission rate estimates. *Atmospheric Environment, 42*, 7373–7383.

Edelmann, W., Schleiss, K., Engeli, H. & Baier, U. (2001). *Ökobilanz der Stromgewinnung aus landwirtschaftlichem Biogas*. Baar, Arbeitsgemeinschaft Bioenergie (arbi)

Flesch, T. K., Wilson, J. D., Harper, L. A., Crenna, B. P., & Sharpe, R. R. (2004). Deducing ground-air emissions from observed trace gas concentrations: a field trial. *Journal of Applied Meteorology, 43*, 487–502.

Flesch, T. K., Wilson, J. D., Harper, L. A., & Crenna, B. P. (2005). Estimating gas emissions from a farm with an inverse-dispersion technique. *Atmospheric Environment, 39*, 4863–4874.

Flesch, T. K., Harper, L. A., Desjardins, R. I., Gao, Z., & Crenna, B. P. (2009). Multi-source emission determination using an inverse-dispersion technique. *Boundary-Layer Meteorology, 132*, 11–30.

Flesch, T. K., Dejardins, R. L., & Worth, D. (2011). Fugitive methane emissions from an agricultural biodigester. *Biomass and Bioenergy, 35*, 3927–3935.

FNR – Fachagentur Nachwachsende Rohstoffe e.V. (2009). Biogas-Messprogramm II – 61 Biogasanlagen im Vergleich. 1st Edn. Fachagentur Nachwachsende Rohstoffe e.V. (Ed) Gülzow. http://groengas.nl/wp-content/uploads/2011/09/messdaten-biogasmessprogramm.pdf Accessed 15 September 2013

Galle, B., Samuelsson, J., Svensson, B., & Borjesson, G. (2001). Measurements of methane emissions from landfills using a time correlation tracer method based on FTIR absorption spectroscopy. *Environmental Science and Technology, 35*, 21–25.

Gentle, J. E. (1998). *Numerical linear algebra for applications in statistics*. New York: Springer. ISBN 0-387-98542-5.

Gerald, C. F., & Wheatley, P. O. (1984). *Applied numerical analysis* (p. 579). Reading: Addison-Wesley Publishing.

Goldsmith, D. C., Chanton, J., Abichou, T., Swan, N., Green, R., & Hater, G. (2012). Methane emissions from 20 landfills across the United States using vertical radial plume mapping. *Journal of the Air & Waste Management Association, 62*(2), 183–197.

Haupt, S. E., Young, G. S., & Allen, C. T. (2006). Validation of a receptor/ dispersion model coupled with a genetic algorithm using synthetic data. *Journal of Applied Meteorology, 45*, 476–490.

Hirtl, M., & Baumann-Stanzer, K. (2007). Evaluation of two dispersion models (ADMS-Roads and LASAT) applied to street canyons in Stockholm, London and Berlin. *Atmospheric Environment, 41*, 5959–5971.

Hirtl, M., Baumann-Stanzer, K., Kaiser, A., Petz, E., & Rau, G. (2007). *Evaluation of three dispersion models for the Trbovlje power plant, Slovenia*. Proc. of the 11th Int. Conf. on harmonization within atmospheric dispersion modeling for regulatory purposes, Cambridge, UK, 2 – 5 July 2007, 21 – 25.

Janicke Consulting, (2011). *Dispersion model LASAT version 3.2 Reference book.*

Liebetrau, J., Clemens, J., Cuhls, C., Hafermann, C., Friehe, J., Weiland, P., & Daniel-Gromke, J. (2010). Methane emissions from biogas-producing facilities within the agricultural sector. Technical Report. *Engineering in Life Science, 10*(6), 595–599.

Liebetrau, J., Reuschel, C., Clemens, J., Hafermann, C., Friehe, J., & Weiland, P. (2011). Analysis of greenhouse gas emissions from 10 biogas plants within the agricultural sector. International Symposium on Anaerobic Digestion of Solid Waste and Energy Crops (ADSW&EC). 28. August – 01. September 2011 in Vienna. Full Paper on CD.

McGinn, S. M., Flesch, T. K., Harper, L. A., & Beauchemin, K. A. (2006). An approach for measuring methane emissions from whole farms. *Journal of Environmental Quality, 35*, 14–20.

McGinn, S. M., Beauchemin, K. A., & Flesch, T. K. (2009). Performance of a dispersion model to estimate methane loss from cattle in pens. *Journal of Environmental Quality, 38*, 1795–1802.

McGinn, S. M., Turner, D., Tomkins, N., Charmley, E., Bishop-Hurley, G., & Chen, D. (2011). Methane emissions from grazing cattle using point-source dispersion. *Journal of Environmental Quality, 40*, 22–27.

Piringer, M., & Baumann-Stanzer, K. (2009). Selected results of a model validation exercise. *Advances in Science and Research, 3*, 13–16.

Reinhold, G., Kohlhase, M., & Gödeke, K. (2010). *Bedeutung verfahrenstechnischer parameter für Biogasausbeute und Restgaspotential*. 4. Rostocker Bioenergieforum 27. – 28.10.2010. http://www.tll.de/ainfo/pdf/biop0111.pdf Accessed 15 September 2013

Roussel, G., Delmaire, G., Ternisien, E., & Lherbier, R. (2000). Separation problem of industrial particles emissions using a stationary scattering model. *Environmental Modeling and Software, 15*, 653–661.

Schatzmann, M., Olesen, H. & Franke, J. (Eds) (2010). *COST 732 model evaluation case studies: approach and results*. 121 pp. COST Office Brussels, ISBN: 3-00-018312-4.

Schauberger, G., Piringer, M., Knauder, W., & Petz, E. (2011). Odour emissions from a waste treatment plant using an inverse dispersion technique. *Atmospheric Environment, 45*, 1639–1647.

Scheutz, C., Samuelsson, J., Fredenslund, A. M., & Kjeldsen, P. (2011). Quantification of multiple methane emission sources at landfills using a double tracer approach. *Waste Management, 31*, 1009–1017.

Siegl, S., Laaber, M., & Holubar, P. (2011). Green electricity from biomass, Part I: Environmental of direct life cycle emissions. *Waste Biomass Valor, 2*, 267–284.

Wilson, J. D., Flesch, T. K., & Bourdin, P. (2010). Ground-air gas emission rate inferred from measured concentration rise, within a disturbed atmospheric surface layer. *Journal of Applied Meteorology, 49*, 1818–1830.

Yee, E. (2008). Theory for reconstruction of an unknown number of contaminant sources using probabilistic inference. *Boundary-Layer Meteorology, 127*(3), 359–394.

Yee, E., & Flesch, T. K. (2010). Inference of emission rates from multiple sources using Bayesian probability theory. *Journal of Environmental Monitoring, 12*(3), 622–634.